



HAL
open science

Predictions for Uranus-moons radio emissions and comparison with Voyager 2/PRA observations

C. K. Louis, L. Lamy, C. M. Jackman, B. Cecconi, S. L. G. Hess

► **To cite this version:**

C. K. Louis, L. Lamy, C. M. Jackman, B. Cecconi, S. L. G. Hess. Predictions for Uranus-moons radio emissions and comparison with Voyager 2/PRA observations. 9th International Workshop on Planetary, Solar and Heliospheric Radio Emissions (PRE 9), Sep 2022, Dublin, Ireland. 10.25546/103106 . insu-04479113

HAL Id: insu-04479113

<https://insu.hal.science/insu-04479113v1>

Submitted on 29 Nov 2024

HAL is a multi-disciplinary open access archive for the deposit and dissemination of scientific research documents, whether they are published or not. The documents may come from teaching and research institutions in France or abroad, or from public or private research centers.

L'archive ouverte pluridisciplinaire **HAL**, est destinée au dépôt et à la diffusion de documents scientifiques de niveau recherche, publiés ou non, émanant des établissements d'enseignement et de recherche français ou étrangers, des laboratoires publics ou privés.



Distributed under a Creative Commons Attribution - NonCommercial - ShareAlike 4.0 International License

PREDICTIONS FOR URANUS-MOONS RADIO EMISSIONS AND COMPARISON WITH VOYAGER 2/PRA OBSERVATIONS

C. K. Louis^{1*} , L. Lamy^{2,3} , C. M. Jackman¹ ,
B. Cecconi² , and S. L. G. Hess⁴ 

*Corresponding author: corentin.louis@dias.ie

Citation:

Louis et al., 2023, Predictions for Uranus-moons radio emissions and comparison with Voyager 2/PRA observations, in *Planetary, Solar and Heliospheric Radio Emissions IX*, edited by C. K. Louis, C. M. Jackman, G. Fischer, A. H. Sulaiman, P. Zucca, published by DIAS, TCD, pp. 421–435, doi: 10.25546/103106

Abstract

Jupiter’s and Saturn’s moons are known to induce auroral emission in the Ultraviolet wavelengths. At Jupiter, the moons Io, Europa and Ganymede are also responsible for powerful decametric radio emissions, driven by the cyclotron maser instability, sustained by weakly relativistic electrons energized through an Alfvénic acceleration process. At Uranus, periodic hectometric radio emissions, observed by the radio instrument Planetary Radio Astronomy experiment of Voyager 2 just after the closest approach of Uranus on 24th Jan. 1986, were tentatively attributed by Kistler (1988) to a similar Alfvénic interaction between the moon Ariel and the planet. Taking advantage of recent prediction and modeling efforts devoted to understand the Jupiter-satellite decametric emissions, and in the context of preparing a future Uranus Orbiter, we calculate an estimate of the theoretical power generated as Alfvén waves by the electrodynamic interaction between Uranus and its three closest large satellites Miranda, Ariel and Umbriel of 10^5 W. We then present simulations of the expected radio emission induced by these moons, using the Exoplanetary and Planetary Radio Emission Simulator (ExPRES). The simulations are compared to the high resolution measurements of the radio instrument onboard Voyager 2 recently refurbished in a digital format. Our conclusion confirms that

¹ School of Cosmic Physics, DIAS Dunsink Observatory, Dublin Institute for Advanced Studies, Dublin 15, Ireland

² LESIA, Observatoire de Paris, Université PSL, CNRS, Sorbonne Université, Université Paris Cité, Meudon, France

³ Aix Marseille Université, CNRS, CNES, LAM, Marseille, France

⁴ ONERA-The French Aerospace Lab, 31055 Toulouse, France

the arc-shaped intermittent structure identified by Kistler (1988) is consistent with emissions induced by the Ariel-Uranus interaction, produced through the cyclotron maser instability driven by a loss cone-type electron distribution function and a resonant electron population of 20 keV.

1 Introduction

Several of Jupiter's and Saturn's conductive moons are known to interact with the strong ambient magnetic field as revealed by Ultraviolet (UV) auroral emissions at the footprint of their magnetic flux tube (Prangé et al., 1996; Clarke, 1998; Clarke et al., 2002; Pryor et al., 2011). At Jupiter, the moons Io, Europa and Ganymede are also known to be responsible for powerful decametric radio emissions (Bigg, 1964; Louis et al., 2017c; Zarka et al., 2017, 2018; Louis et al., 2020; Jácome et al., 2022). At Saturn, a similar search for Saturn-Enceladus kilometric emissions turned to be unsuccessful so far (Viévard, 2012).

Much like Earth's auroral kilometric radiation (AKR, Wu & Lee, 1979; Le Queau et al., 1984b,a; Pritchett, 1986; Wu, 1985; Treumann, 2006), Saturn's kilometric radiation (SKR, e.g., Kaiser & Desch, 1984; Lamy et al., 2008a; Lamy, 2017; Lamy et al., 2018) and Jupiter's moon-independent auroral kilometric, hectometric and decametric radio emissions (Louarn et al., 2017, 2018; Collet et al., 2023, this issue), these moon-induced radio emissions have been shown to be driven by the Cyclotron Maser Instability (CMI) from loss cone electron distributions functions of a few keV, sustained by an Alfvénic acceleration process (Hess et al., 2008; Louis et al., 2020). The CMI is a wave-electron instability for which the resonance condition is reached when the Doppler-shifted angular frequency of the wave in the frame of the electron ($\omega - k_{\parallel}v_{r\parallel}$) is equal to the relativistic gyration frequency of the resonant electrons ($\omega_{ce}\Gamma_r^{-1}$):

$$\omega = 2\pi f = \omega_{ce}\Gamma_r^{-1} + k_{\parallel}v_{r\parallel} \quad (1)$$

In this equation, the \parallel index refers to the component parallel to the magnetic field line, k is the wave vector, v_r the resonant electron velocity, and $\Gamma_r^{-1} = \sqrt{1 - v_r^2/c^2}$ the Lorentz factor associated with the motion of resonant electrons (Wu & Lee, 1979; Le Queau et al., 1984b,a; Pritchett, 1986; Wu, 1985; Treumann, 2006). The CMI efficiently amplifies X-mode emissions at frequencies very close to the electron cyclotron angular frequency $\omega_{ce} = 2\pi f_{ce}$ (directly proportional to the local magnetic field B).

At Uranus, the only radio observations we have are those recorded by the Planetary Radio Astronomy radio instrument (PRA, Warwick et al., 1977) on board the Voyager 2 mission (see Figure 1). The strongest emissions were observed between 15 and 850 kHz, with a high degree of circular polarisation, strongly comparable to that of the AKR and SKR, although an order of magnitude weaker. They have thus been attributed to the CMI mechanism and called Uranian Kilometric Radiation (UKR) by analogy with the AKR and SKR emissions. Moreover, these emissions were measured as being preferentially directed towards the night side of the magnetosphere. Because of Voyager's trajectory (arrival on the day side, departure on the night side) they were detected only 5 days before

the closest approach on 24th January 1986, but up to 1 month later (Warwick et al., 1986; Leblanc et al., 1987; Kaiser, 1988; Desch et al., 1991; Farrell et al., 1991; Farrell, 1992; Lamy et al., 2023, this issue).

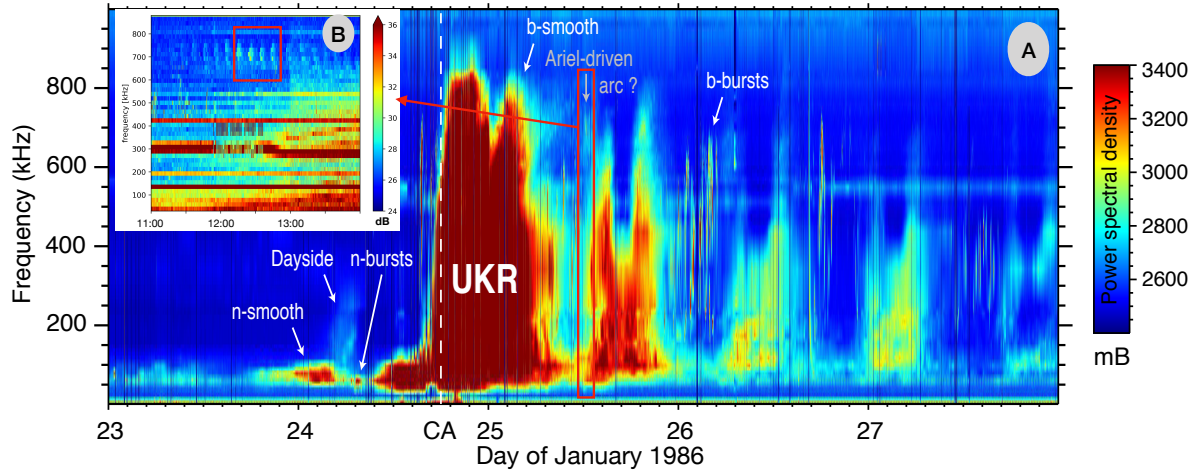


Figure 1: Dynamic spectrum of Voyager 2/PRA observation around the Uranus closest approach on 24th January 1986. We note the linear y-axis scale, which reveals the spread of UKR over a range from ~ 50 -800 kHz, sub-divided in five components: narrowband (n-) and broadband (b-) burst or smooth emissions, and potential Ariel-induced kilometric emissions (see insert (B) for a closest zoom-in on these emissions). We also note that most of the emissions are visible after the closest approach (CA), hence from the nightside of the magnetosphere, while only low-frequency emissions are visible from the dayside. For more details on each components, please see Lamy et al. (2023, this issue, of which panel (A) is from)

The UKR is divided into different components, such as the narrowband (n-) and broadband (b-) smooth or burst emissions, all visible in Figure 1. For more details on each of these emissions, please refer to Lamy et al. (2023, this issue). Here, we will focus on the component of the UKR, labelled “Ariel-driven arc?”, a zoom on which is visible in the insert, displaying high-frequency arc structures in the [600-800] kHz frequency range with a 10 minute periodicity. Kistler (1988) tentatively attributed this periodic signature of hectometric radio emissions to an Alfvénic interaction between the moon Ariel and the planet.

Therefore, in the context of preparing a future Uranus Orbiter in general, and the re-exploration of the Uranus radio spectrum in particular (see Lamy et al., 2023, this issue), we present here a theoretical study on the radio emissions that could be induced by the interactions between Uranus and its moons Miranda, Ariel and Umbriel. We choose these three moons because they are the largest and closest to Uranus of the Uranian moons, and because there is evidence of plasma confined close to the magnetic equator between Miranda and Ariel (Mauk et al., 1987; Cohen et al., 2023), which is thought to be due to these moons. The next two moons, Titania and Oberon, are assumed to be at too great an orbital distance and too close to the magnetopause (Cheng, 1987; Arridge & Paty, 2021).

In Section 2 we recall the context of the measurements recorded by Voyager/PRA. In Section 3, based on radio, plasma and magnetic measurements from different instruments

onboard Voyager 2, we calculate the total power generated by the Uranus-satellite electrodynamic interaction by re-applying the method developed by Hess et al. (2011) for the cases of Jupiter and Saturn. In Section 4, we perform a parametric study of simulations of the expected Uranian moon-induced radio emissions, using the Exoplanetary and Planetary Radio Emission Simulator (ExPRES, Louis et al., 2019), successfully used to discover Jupiter-Europa and -Ganymede decametric emissions in Cassini and Voyager observations (Louis et al., 2017c). The simulations are then compared to the Voyager 2/PRA high resolution data recently refurbished in a digital format (Cecconi et al., 2017).

2 Flyby trajectory and *in situ* measurements

In January 1986, the Voyager 2 spacecraft performed the only and unique flyby of Uranus. The rapid trajectory of Voyager 2 through the magnetic meridional plane of Uranus' magnetosphere on 24th January 1986 is displayed in Figure 2. The moon minimum L shells (normalized distance at the equator) for the closest Uranian moon Miranda, Ariel and Umbriel are shown. Note here that this is the *minimum* L-shell, because the moons orbit in the plane of the rotational equator, not in the plane of the magnetic equator, therefore the magnetic field lines connected to the moons change during the rotation.

Voyager 2 acquired pioneer *in situ* measurements within the Uranian magnetosphere, such as the electron and ions density measured along the spacecraft trajectory by the “plasma science experiment” (PLS, Bridge et al., 1977) and the “low energy charged particle experiment” (LECP, Krimigis et al., 1977) instruments. During the flyby, the spacecraft was in the plane of the ecliptic, and therefore crossed the magnetic field lines connected to the moons at non-zero magnetic latitudes, and different for each moon (see L_{\min} annotations in Figure 2). During the crossings of the Uranian moons L-Shell, an increase in the electron and ions (mainly protons) density was measured (Mauk et al., 1987; Sittler et al., 1987). At that time, between 19:00 and 22:00, the spacecraft was undergoing a charging event, due to enhanced fluxes of keV electrons (Sittler et al., 1987). During this event, the spacecraft was charged negatively (potentials between -28 V and -400 V). This results in a deceleration of the electrons. As a result, thermal electrons cannot penetrate the potential barrier surrounding the spacecraft and be detected, which could explain why the instruments detect a lower electron density than the ion density. We therefore take the ions measurements (both from LECP and PLS instruments), and make the assumption that, due to quasi-neutrality, the electron density should be the same. These values are given in Table 1 (second and third columns).

Planet-satellite interactions occur when an electrically conductive moon moves in a strong magnetic field and plasma environment. Based on Mauk et al. (1987) and the recent work of Cohen et al. (2023), there is evidence of a dense populations of ions and electrons confined particularly close to the magnetic equator between the L-shell of Miranda and Ariel moons. Therefore, the plasma conditions could be met at these two moons to provide a conductive environment for Alfvénic perturbations to arise, and for radio emissions to be produced along the flux tube that links these moons to Uranus.

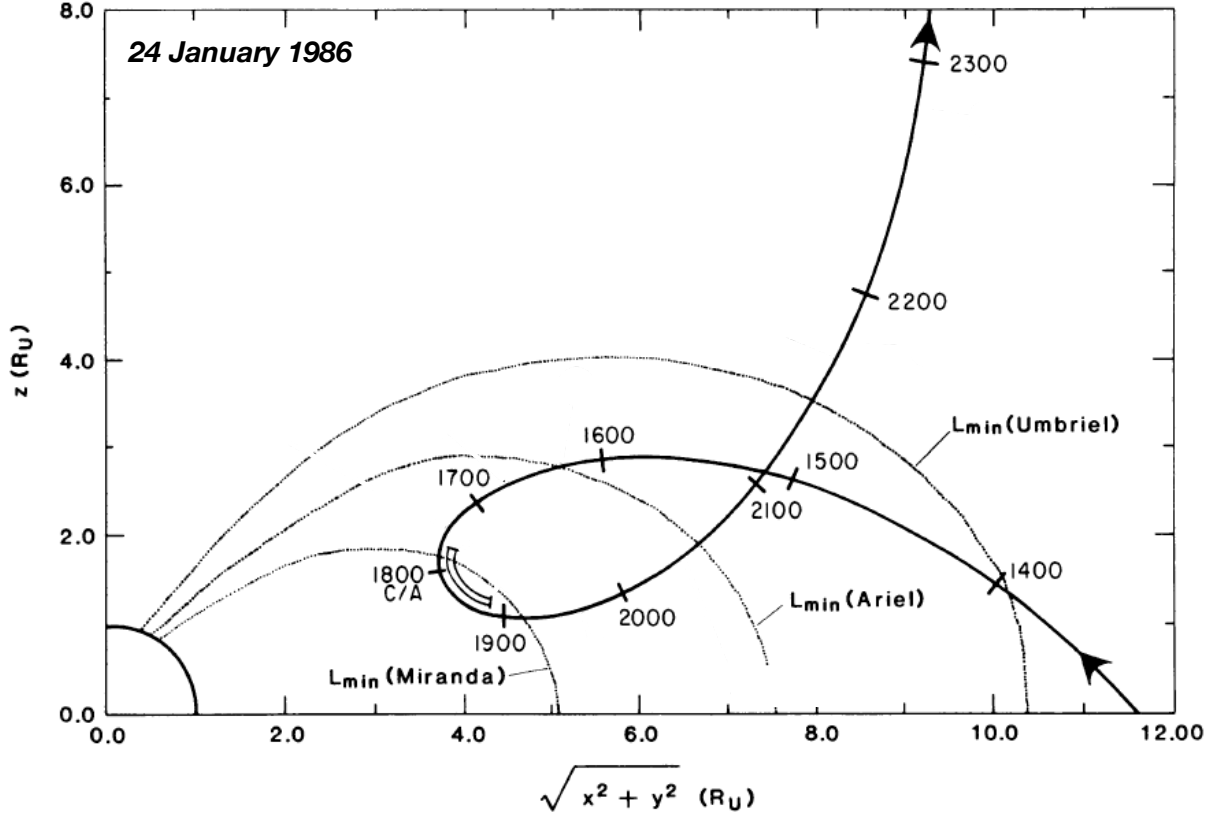


Figure 2: Trajectory of Voyager in the Uranus magnetic meridional plane (based on Ness et al., 1986, magnetic field model) around the closest approach (CA) on 24th January 1986. The moon minimum L shells for Miranda, Ariel and Umbriel are shown. [Figure adapted from Bridge et al. (1986); Sittler et al. (1987). Note that in Sittler et al. (1987), the Figure is erroneously dated 25th January 1986.]

3 Theoretical generated power

In this section, we summarise the main equations, developed by Hess et al. (2011) for the cases of Jupiter's and Saturn's moons, which allow to calculate the total power generated by planet-satellite electrodynamic interaction from Ohm's voltage-current relationship (Neubauer, 1980; Goertz, 1983; Saur, 2004). We then apply this method to the (much more complicated) case of Uranian moons.

The power radiated as Alfvén waves by moon-planet interaction can be written as:

$$P \sim 4E_{moon}^2 R_{moon}^2 \Sigma_{\text{Alfven}} \quad (2)$$

In this equation, R_{moon} is the radius of the moon. E_{moon} is the electric field, in the moon reference frame, generated by the relative motion of the moon v_{moon} inside a magnetic field B and a plasma environment:

$$E_{moon} = -v_{moon} \times \mathbf{B} \quad (3)$$

Finally, Σ_{Alfven} is the Alfvén conductance along the moon's orbit:

$$\Sigma_{\text{Alfven}} = \sqrt{\frac{\rho}{\mu_0 B^2}} \quad (4)$$

with μ_0 the vacuum permeability and ρ the mass density of the plasma, i.e.:

$$\rho = m_e n_e + \sum_i^N (m_i n_i) \quad (5)$$

with (m_e, n_e) and (m_i, n_i) the mass and density (in m^{-3}) of electrons and ions species, respectively. In this present case, the ions species are only protons H^+ .

Therefore, to calculate the power generated at the Uranian moons, it is mandatory to determine the values of the magnetic field and the densities $n_{e_{\text{moons}}}$ and $n_{H^+_{\text{moons}}}$ at the moons (see Table 1 third column). To calculate these densities ($n_{e_{\text{moons}}}, n_{H^+_{\text{moons}}}$), we rely on the density measurements obtained by Voyager (see Table 1 second column) along its trajectory when crossing the flux tubes connected to the moons, and on the Bagenal (1994) torus plasma diffusion equation:

$$n_{\text{species}} = n_{\text{species}_{\text{moon}}} \exp\left(-\frac{\sqrt{(r-r_0)^2 + z^2}}{H}\right) \quad (6)$$

where r_0 is the torus center equatorial diameter, H the torus scale-height (taken as equal to 1), $n_{\text{species}_{\text{moon}}}$ the reference plasma number density at the moon, and n_{species} the density value at a given equatorial radial distance $r = \sqrt{x^2 + y^2}$ and a given altitude above equator z . All distance units are expressed in planetary radius ($R_{\text{Uranus}} = 25559$ km). The torus center equatorial diameter r_0 is taken at $6 R_{\text{Uranus}}$, based on Mauk et al. (1987); Cohen et al. (2023). Although, of course, this calculation is probably far from providing exact values, it gives a first-order estimate of the power generated at the moons, in the conditions of Voyager 2 flyby.

Once the electrons $n_{e_{\text{moon}}}$ and ions $n_{H^+_{\text{moon}}}$ densities at the moon are obtained, the Alfvén conductance Σ_{Alfven} can be calculated based on Equation 4. Using the velocity of the moon in Uranus frame v_{moon} , the magnetic field values (based on Ness et al., 1986), and Equation 3, we determine the induced electric field E_{moon} . Finally, using Equation 2 and the moons radius R_{moon} , we calculate the estimated power P generated at the moons (see Table 1).

The values of power obtained, of the order of 10^5 W, must of course be treated with caution, since they are not based on *in situ* measurements of the plasma at the moons, but on single values along the flux tubes and on a plasma diffusion equation for a torus. However, these values give us an order of magnitude estimate (the best possible with the current data) of what the lower limit of the power generated at these moons might be. If we compare them to the values obtained for Io, Europa and Enceladus (Hess et al., 2011), they are order of magnitude below the values at those three moons. Thus, the intensity of radio emissions induced by these moons would be extremely weak.

The next step is however to consider the observational consequences of such induced radio emissions, which is especially timely given the planned *in situ* exploration of the Uranian system in the next decades.

Table 1: This table gives, for the Uranian moons Miranda, Ariel and Umbriel, the electron $n_{e \text{ Voyager}}$ and $H^+ n_{H^+ \text{ Voyager}}$ densities measured by Voyager PLS (1 Mauk et al., 1987) and LECP (2 Sittler et al., 1987), the estimated electron $n_{e \text{ moon}}$ and $H^+ n_{H^+ \text{ moon}}$ densities at the moon, the magnetic field value at the moons B_{moon} (based on [3] Ness et al., 1986, magnetic field model), the Alfvén conductance Σ_{Alfven} , the velocity of the moon v_{moon} along its orbit ([4] Stone & Miner, 1986), the electric field at the moon E_{moon} , the moon radius R_{moon} ([4] Stone & Miner, 1986) and the estimated power P generated at the moon.

Satellite	$n_{e \text{ Voyager}}^{[1,2]}$ (cm^{-3})	$n_{H^+ \text{ Voyager}}^{[1,2]}$ (cm^{-3})	$n_{e \text{ moon}}$ (cm^{-3})	$n_{H^+ \text{ moon}}$ (cm^{-3})	$B_{\text{moon}}^{[3]}$ (nT)	Σ_{Alfven} (Ω^{-1})	$v_{\text{moon}}^{[4]}$ (km.s^{-1})	E_{moon} (V.km^{-1})	$R_{\text{moon}}^{[4]}$ (km)	P (W)
Miranda	1×10^0	1×10^0	5.5	5.5	215.6	0.4	6.5	-1.5	242	$\sim 2 \times 10^5$
Ariel	4×10^{-1}	4×10^{-1}	3.1	3.1	47.3	1.4	13.8	-0.26	580	$\sim 10^5$
Umbriel	3×10^{-1}	3×10^{-1}	7.9	7.9	35.6	2.9	22.3	-0.16	595	$\sim 10^5$

4 Simulations

In this section, we present the main results of the parametric study of the simulations of radio emissions induced by the moons Miranda, Ariel and Umbriel using the ExPRES code.

The ExPRES code (Hess et al., 2008; Louis et al., 2019) computes the geometrical visibility of radio sources around a magnetized planet and tests at each time/frequency step whether the radiated waves are visible or not for a given observer. This visibility depends in particular on the radio beaming angle, i.e., the aperture angle $\theta = (\mathbf{B}, \mathbf{k})$ between the magnetic field vector at the source and the emitted wave vector. This angle is computed in a self-consistent way in the frame of the CMI theory (see Equation 1), based on the choice of the electron distribution that drives the emission: loss cone distribution produces oblique emission with variable $\theta(f)$, whereas ring/shell distribution produces perpendicular emission ($\theta \sim 90^\circ$) at all frequencies. ExPRES simulations are then used to produce time-frequency spectrograms (or dynamic spectrum) of visible radio sources which can be directly compared to observations.

Such simulations have been employed to study radio emissions of Jupiter (e.g., Hess et al., 2008; Cecconi et al., 2012, 2021), Saturn (e.g., Lamy et al., 2008b, 2013), exoplanets (Hess & Zarka, 2011) and successfully used to discover radio emission induced by the Jupiter’s moons Europa and Ganymede (Louis et al., 2017c).

In practice, to set up an ExPRES simulation, we define (1) the magnetic and plasma environment around the planet, (2) the spatial distribution of point radio sources, (3) the electron distribution function to calculate the emission angle θ , and (4) the location of the observer.

In this study, we used (1) the Herbert (2009) AH5 (for “Auroral Hexadecapole L = 5”) magnetic field model. (2) The active magnetic field lines are those connected to the moons, i.e. L = 5.1 for Miranda, 7.5 for Ariel and 10.4 for Umbriel. (3) We choose here a loss cone electron distribution function, as it is the one that has been detected *in situ*

for the emissions induced by Io, Europa and Ganymede (Louis et al., 2020, 2023) and that allows to simulate most accurately these same emissions with ExPRES (Louis et al., 2017b,c). Finally, (4) the position of the observer is set at Voyager 2 position.

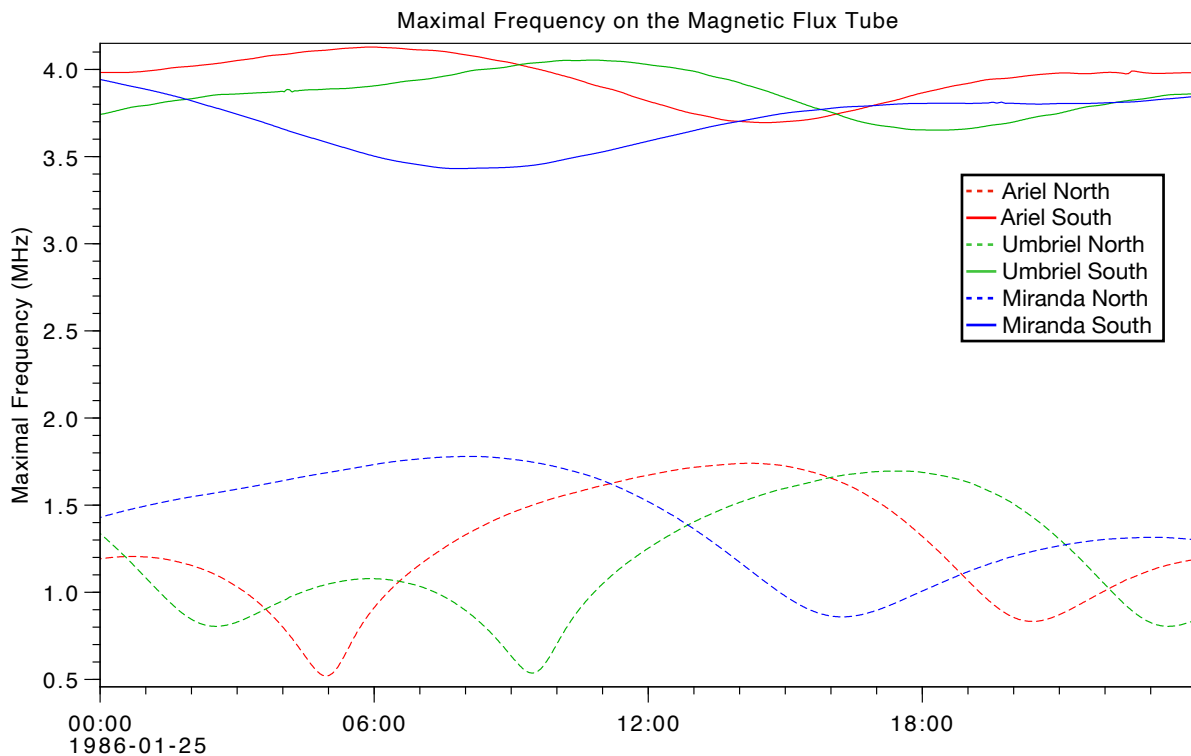


Figure 3: Maximal frequency on the magnetic flux tubes associated with the Uranian moons. Solid lines (at higher frequencies) represent the southern hemisphere while dashed lines (at lower frequencies) are for northern hemisphere. Red lines are for Ariel, green lines for Umbriel and blue lines for Miranda. The magnetic field model used is the Herbert (2009) AH5 model.

Figure 3 displays the expected maximal frequencies reachable by emissions induced by the three moons, in the southern (solid lines) and northern (dashed lines) hemispheres. This figure shows that the theoretical maximum frequencies of the radio emissions induced by the different moons are very different from one hemisphere to another. This is due to the large offset of the magnetic field from the centre of Uranus (~ 0.4 planetary radius). In the north, radio emissions cannot exceed 1.5 MHz, while they can reach 4.0 MHz in the southern hemisphere.

Based on previous works showing that moon-induced radio emissions are produced by a loss cone-type electron distribution function (Louis et al., 2017a,b, 2020, 2023), we do not show here simulations produced from a shell-type function. We produced a set of simulations using different electron energies ($E = 0.1, 1, 5, 10$ and 20 keV). Emissions are produced in both hemisphere. The results of the simulations are shown Figure 4 (panels B-D, along simultaneous Voyager / PRA radio measurements (panel A)).

Radio emissions suspected to be induced by Ariel (Kistler, 1988) are visible between 12h15 and 12h45 at 0.6 MHz, in the form of “spots” that are repeated \sim seven times. Only the four most intense were seen by Kistler (1988), and the temporal separation between

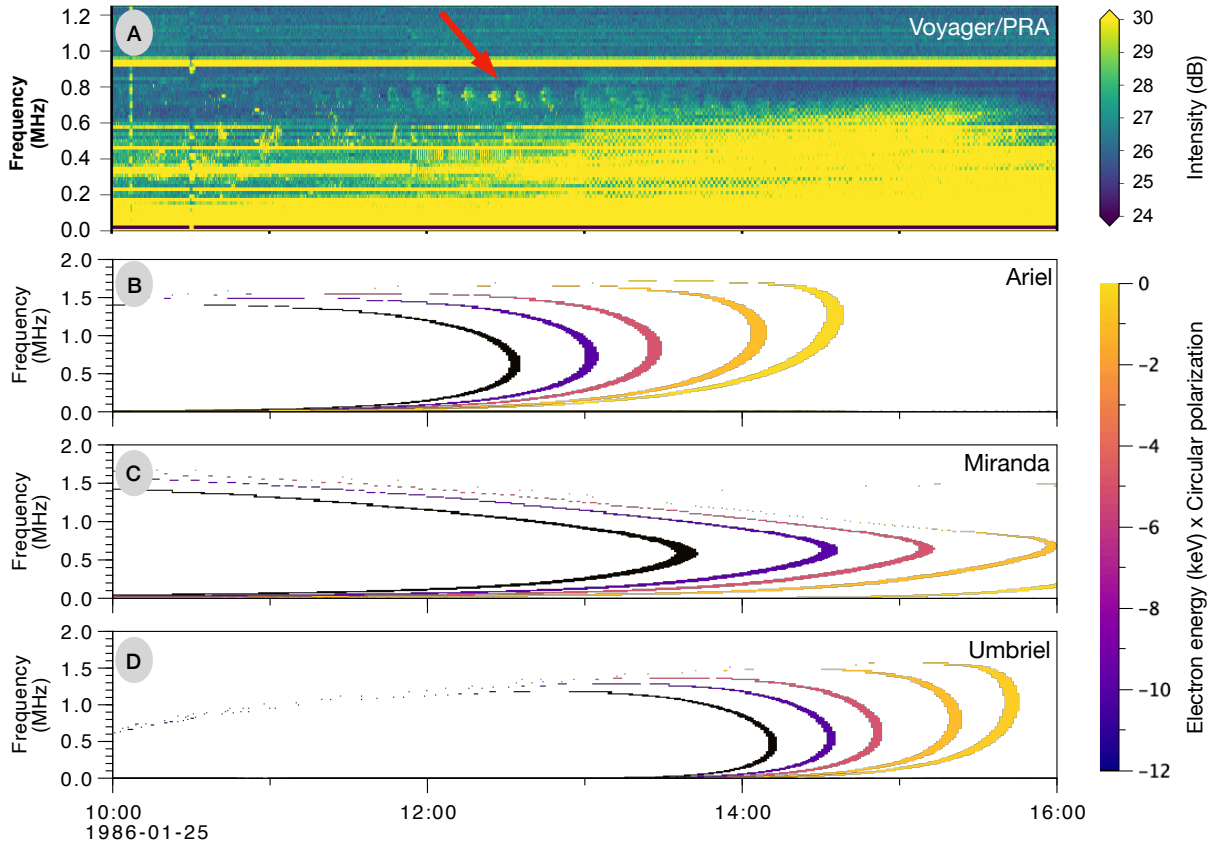


Figure 4: (A) *Voyager 2/PRA* observations, and *ExPRES* simulations for (B) *Ariel*, (C) *Miranda* and (D) *Umbriel* induced radio emissions. The colour bar indicates the electron energy (in keV) used for the simulation, multiplied by the circular polarisation (here -1 , emissions fully circularly polarised, produced in the northern magnetic hemisphere).

them was postulated to be consistent with Alfvén bouncing time between *Ariel* and the ionosphere of *Uranus* (with the assumption of excitation of the Alfvén waves by a unipolar induction, with multiple arcs due to reflection on the planet’s ionosphere). The frequency extension of the observed radio emissions are compatible with northern emission.

The simulations (Figures 4B-D) show that on 25th January 1986, only northern emissions are visible from *Voyager* point of view (circular polarization < 0 , i.e. Right-Handed polarization). If we consider that each “spot” observed in panel A is part of a different arc, the only simulated emissions that are compatible with the observed radio emissions are *Ariel* induced radio emission, both *Miranda* and *Umbriel* radio emissions happen later. The simulation with 20 keV electrons produced the closest fit in time and frequency for the first arc, corresponding to the emission produced in the flux tube connected to *Ariel*. The other arcs would be produced by the bouncing of the Alfvén wave along the plasma layer that would be present along the orbit of *Ariel* (Kistler, 1988).

However, an emission observed in a very narrow spectral band, with so many repetitions (at least seven here) is a bit unique, if compared to multiple radio emissions induced by *Io*. An other possibility is that all the observed “spots” here are the same arc, with an horizontal “envelope”, in which case the periodicity would be due to a modulation of

the interaction along the same flux tube. If so, the simulations that would best fit the observation radio emission will be Miranda-induced emissions, with an electron energy $E_e \geq 20$ keV.

In both case, this electron energy is in agreement with *in situ* measurements made by Voyager 2/PLS, which measured electrons in the 20-35 keV range confined between the orbits of Miranda and Ariel (Mauk et al., 1987).

5 Summary and perspectives

Based on Voyager measurements we have calculated the estimated power dissipated as Alfvén waves by the planet-satellite interaction at the Uranian moons Miranda, Ariel and Umbriel. These values ($\sim 10^5$ W) are order of magnitude below those at Io and Europa (10^{12} W and 10^{11} W, respectively, Hess et al., 2011), where moon-induced UV and radio signatures have been unambiguously observed, and even below that at Enceladus (10^8 W Hess et al., 2011), where not clear detection has been made (Viévard, 2012).

However, these values were calculated using ions and electron densities estimated from a plasma density diffusion equation based on a torus distribution density and from a single measurements per moon along the Voyager trajectory. These density values are therefore not *in situ* values at the moons. These values must then be taken with caution. Simulation of the plasma diffusion and distribution should be run, to have a better estimation of the plasma density at the moons' orbit, but this is a significant piece of research and is outside the scope of this current work.

One should also note that the round-trip time of the Alfvén wave between the satellites and the planet may be shorter than the transit time of a field line through the satellite, in which case the current circuit may not be Alfvén but a unipolar inductor (Goldreich & Lynden-Bell, 1969), in which case the radio sources would potentially be shell-like (as for the Terrestrial auroral kilometric radiation in cavities), rather than loss cones, leading to purely perpendicular emissions.

Based on ExPRES simulations, induced radio emission by the different moons could reach 1.5 MHz (Northern magnetic hemisphere) to 4.0 MHz (Southern magnetic hemisphere). Finally, by comparing the radio emissions identified by Kistler (1988) as Ariel-induced emissions and the ExPRES simulations, we have shown that the direction of curvature of the emissions, the occurrence in time and the extension in frequency of the radio emissions could be compatible with only Ariel- or Miranda-induced radio emissions produced in the northern magnetic hemisphere, depending on the nature of these multiple spots, depending on whether they are different structures (multiple arcs from Alfvén waves bouncing between Uranus' ionosphere and Ariel) or part of the same envelope (with a periodicity due to the modulation of the interaction in the flux tube). Emissions induced by Umbriel happen too late and are therefore not a possible origin of these emissions. With a single observation, it is therefore difficult to draw a clear conclusion on the origin of these emissions. It does, however, provide new constraints on their possible origin, such as the magnetic hemisphere of origin and the energy of the electrons.

Depending on the configuration of the magnetosphere with respect to the solar wind, the plasma confined between Miranda's and Ariel's orbit (Mauk et al., 1987; Cohen et al., 2023) could be dense enough to have a stronger Alfvénic conductance, allowing radio emissions to be sporadically produced. From then on, their statistical search with a potential future orbiter will be possible, and would allow to enlarge the number of cases of planet-satellite interactions inducing radio emissions.

Acknowledgments

C. K. Louis' and C. M. Jackman's work at the Dublin Institute for Advanced Studies was funded by the Science Foundation Ireland Grant 18/FRL/6199. French co-authors acknowledge the support from CNES and CNRS/INSU programs of planetology and heliophysics.

References

- Arridge C. S., Paty C., 2021, Asymmetrical Magnetospheres: Uranus and Neptune, *in Magnetospheres in the Solar System*, p. 515, doi:10.1002/9781119815624.ch33
- Bagenal F., 1994, Empirical model of the Io plasma torus: Voyager measurements, *Journal of Geophysical Research*, 99, 11043
- Bigg E. K., 1964, Influence of the Satellite Io on Jupiter's Decametric Emission, *Nature*, 203, 1008
- Bridge H. S., Belcher J. W., Butler R. J., Lazarus A. J., Mavretic A. M., Sullivan J. D., Siscoe G. L., Vasyliunas V. M., 1977, The Plasma Experiment on the 1977 Voyager Mission, *Space Science Reviews*, 21, 259
- Bridge H. S., et al., 1986, Plasma Observations near Uranus: Initial Results from Voyager 2, *Science*, 233, 89
- Cecconi B., et al., 2012, Natural radio emission of Jupiter as interferences for radar investigations of the icy satellites of Jupiter, *Planetary Space Science*, 61, 32
- Cecconi B., Pruvot A., Lamy L., Zarka P., Louis C., Hess S. L. G., Evans D. R., Boucon D., 2017, Refurbishing Voyager 1 & 2 Planetary Radio Astronomy (PRA) data, *in Planetary Radio Emissions VIII*, eds Fischer, G. and Mann, G. and Panchenko, M. and Zarka, P., pp 505–514, doi:10.1553/PRE8s505
- Cecconi B., Louis C. K., Muñoz Crego C., Vallat C., 2021, Jovian auroral radio source occultation modelling and application to the JUICE science mission planning, *Planetary Space Science*, 209, 105344
- Cheng A. F., 1987, Proton and oxygen plasmas at Uranus, *Journal of Geophysical Research*, 92, 15309

- Clarke J. T., 1998, Hubble space telescope imaging of jupiter's uv aurora during the galileo orbiter mission, *Journal of Geophysical Research: Planets*, 103, 20217
- Clarke J. T., et al., 2002, Ultraviolet emissions from the magnetic footprints of Io, Ganymede and Europa on Jupiter, *Nature*, 415, 997
- Cohen I. J., Turner D. L., Kollmann P., Clark G. B., Hill M. E., Regoli L. H., Gershman D. J., 2023, A Localized and Surprising Source of Energetic Ions in the Uranian Magnetosphere Between Miranda and Ariel, *Geophysical Research Letters*, 50, e2022GL101998
- Collet B., Lamy L., Louis C. K., Zarka P., Prangé P., Louarn P., Sulaiman A., Kurth W. S. K., 2023, Characterization of Jovian hectometric sources with Juno: statistical position and generation by shell-type electrons, in *Planetary, Solar and Heliospheric Radio Emissions IX*, eds Louis, C. K. and Jackman, C. M. and Fischer, G. and Sulaiman, A. H. and Zucca, P., DIAS and TCD, doi:10.25546/103095
- Desch M. D., Kaiser M. L., Zarka P., Lecacheux A., Leblanc Y., Aubier M., Ortega-Molina A., 1991, Uranus as a radio source., in *Uranus*, eds Bergstrahl, Jay T. and Miner, Ellis D. and Matthews, Mildred S., pp 894–925
- Farrell W. M., 1992, Nonthermal radio emissions from Uranus, in *Planetary Radio Emissions III*, eds Rucker, H. O. and Bauer, S. J. and Kaiser, M. L., pp 241–269
- Farrell W. M., Desch M. D., Kaiser M. L., Calvert W., 1991, Evidence of auroral plasma cavities at Uranus and Neptune from radio burst observations, *Journal of Geophysical Research*, 96, 19049
- Goertz C. K., 1983, The Io-control of Jupiter's decametric radiation: The Alfvén wave model, *Advances in Space Research*, 3, 59
- Goldreich P., Lynden-Bell D., 1969, Io, a jovian unipolar inductor, *Astrophysical Journal*, 156, 59
- Herbert F., 2009, Aurora and magnetic field of Uranus, *Journal of Geophysical Research (Space Physics)*, 114, A11206
- Hess S. L. G., Zarka P., 2011, Modeling the radio signature of the orbital parameters, rotation, and magnetic field of exoplanets, *Astronomy & Astrophysics*, 531, A29
- Hess S., Cecconi B., Zarka P., 2008, Modeling of Io-Jupiter decameter arcs, emission beaming and energy source, *Geophysical Research Letters*, 35, L13107
- Hess S. L. G., Delamere P. A., Dols V., Ray L. C., 2011, Comparative study of the power transferred from satellite-magnetosphere interactions to auroral emissions, *Journal of Geophysical Research (Space Physics)*, 116, A01202
- Jácome H. R. P., Marques M. S., Zarka P., Echer E., Lamy L., Louis C. K., 2022, Search for Jovian decametric emission induced by Europa on the extensive Nançay Decameter Array catalog, *Astronomy & Astrophysics*, 665, A67

- Kaiser M. L., 1988, Uranus radio emissions, in *Planetary Radio Emissions II*, eds Rucker, H. O. and Bauer, S. J. and Pedersen, B. M., pp 195–213
- Kaiser M. L., Desch M. D., 1984, Radio emissions from the planets earth, Jupiter, and Saturn., *Reviews of Geophysics and Space Physics*, 22, 373
- Kistler A. C., 1988, Voyager 2 Detection of Uranian Hectometric Radio Arcs, https://space.physics.uiowa.edu/~dag/theses_docs/Kistler_MS_1988_r.pdf
- Krimigis S. M., Armstrong T. P., Axford W. I., Bostrom C. O., Fan C. Y., Gloeckler G., Lanzerotti L. J., 1977, The Low Energy Charged Particle (LECP) Experiment on the Voyager Spacecraft, *Space Science Reviews*, 21, 329
- Lamy L., 2017, The Saturnian kilometric radiation before the Cassini Grand Finale, in *Planetary Radio Emissions VIII*, eds Fischer, G. and Mann, G. and Panchenko, M. and Zarka, P., pp 171–190, doi:10.1553/PRE8s171
- Lamy L., Zarka P., Cecconi B., Prangé R., Kurth W. S., Gurnett D. A., 2008a, Saturn kilometric radiation: Average and statistical properties, *Journal of Geophysical Research (Space Physics)*, 113, A07201
- Lamy L., Zarka P., Cecconi B., Hess S., Prangé R., 2008b, Modeling of Saturn kilometric radiation arcs and equatorial shadow zone, *Journal of Geophysical Research (Space Physics)*, 113, A10213
- Lamy L., et al., 2013, Multispectral simultaneous diagnosis of Saturn’s aurorae throughout a planetary rotation, *Journal of Geophysical Research (Space Physics)*, 118, 4817
- Lamy L., et al., 2018, The low-frequency source of Saturn’s kilometric radiation, *Science*, 362, aat2027
- Lamy L., et al., 2023, Re-exploring the radio spectrum of Uranus in orbit: science case and digital high-frequency receiver, in *Planetary, Solar and Heliospheric Radio Emissions IX*, eds Louis, C. K. and Jackman, C. M. and Fischer, G. and Sulaiman, A. H. and Zucca, P., DIAS and TCD, doi:10.25546/103105
- Le Queau D., Pellat R., Roux A., 1984a, Direct generation of the auroral kilometric radiation by the maser synchrotron instability: An analytical approach, *Physics of Fluids*, 27, 247
- Le Queau D., Pellat R., Roux A., 1984b, Direct generation of the auroral kilometric radiation by the maser synchrotron instability: Physical mechanism and parametric study, *Journal of Geophysical Research*, 89, 2831
- Leblanc Y., Aubier M. G., Ortega-Molina A., Lecacheux A., 1987, Overview of the uranian radio emissions: Polarization and constraints on source locations, *Journal of Geophysical Research*, 92, 15125
- Louarn P., et al., 2017, Generation of the Jovian hectometric radiation: First lessons from Juno, *Geophysical Research Letters*, 44, 4439

- Louarn P., et al., 2018, Observation of Electron Conics by Juno: Implications for Radio Generation and Acceleration Processes, *Geophysical Research Letters*, *45*, 9408
- Louis C., Lamy L., Zarka P., Cecconi B., Hess S. L. G., Bonnin X., 2017a, Simulating Jupiter-satellite decametric emissions with ExPRES: A parametric study, in *Planetary Radio Emissions VIII*, pp 59–72, doi:10.1553/PRE8s59
- Louis C. K., et al., 2017b, Io-Jupiter decametric arcs observed by Juno/Waves compared to ExPRES simulations, *Geophysical Research Letters*, *44*, 9225
- Louis C. K., Lamy L., Zarka P., Cecconi B., Hess S. L. G., 2017c, Detection of Jupiter decametric emissions controlled by Europa and Ganymede with Voyager/PRA and Cassini/RPWS, *Journal of Geophysical Research (Space Physics)*, *122*, 9228
- Louis C. K., Hess S. L. G., Cecconi B., Zarka P., Lamy L., Aicardi S., Loh A., 2019, ExPRES: an Exoplanetary and Planetary Radio Emissions Simulator, *Astronomy & Astrophysics*, *627*, A30
- Louis C. K., Louarn P., Allegrini F., Kurth W. S., Szalay J. R., 2020, Ganymede-Induced Decametric Radio Emission: In Situ Observations and Measurements by Juno, *Geophysical Research Letters*, *47*, e90021
- Louis C. K., et al., 2023, Source of radio emissions induced by the Galilean moons Io, Europa and Ganymede: In situ measurements by Juno, *Journal of Geophysical Research: Space Physics*, *128*, e2023JA031985
- Mauk B. H., Krimigis S. M., Keath E. P., Cheng A. F., Armstrong T. P., Lanzerotti L. J., Gloeckler G., Hamilton D. C., 1987, The hot plasma and radiation environment of the Uranian magnetosphere, *Journal of Geophysical Research*, *92*, 15283
- Ness N. F., Acuna M. H., Behannon K. W., Burlaga L. F., Connerney J. E. P., Lepping R. P., Neubauer F. M., 1986, Magnetic Fields at Uranus, *Science*, *233*, 85
- Neubauer F. M., 1980, Nonlinear standing Alfvén wave current system at Io - Theory, *Journal of Geophysical Research*, *85*, 1171
- Prangé R., Rego D., Southwood D., Zarka P., Miller S., Ip W., 1996, Rapid energy dissipation and variability of the Io-Jupiter electrodynamic circuit, *Nature*, *379*, 323
- Pritchett P. L., 1986, Cyclotron maser radiation from a source structure localized perpendicular to the ambient magnetic field, *Journal of Geophysical Research*, *91*, 13569
- Pryor W. R., et al., 2011, The auroral footprint of Enceladus on Saturn, *Nature*, *472*, 331
- Saur J., 2004, A model of Io's local electric field for a combined Alfvénic and unipolar inductor far-field coupling, *Journal of Geophysical Research (Space Physics)*, *109*, A01210
- Sittler Edward C. J., Ogilvie K. W., Selesnick R., 1987, Survey of electrons in the Uranian magnetosphere: Voyager 2 observations, *Journal of Geophysical Research*, *92*, 15263

- Stone E. C., Miner E. D., 1986, The Voyager 2 Encounter with the Uranian System, *Science*, *233*, 39
- Treumann R. A., 2006, The electron-cyclotron maser for astrophysical application, *Astronomy & Astrophysics*, *13*, 229
- Viévard S., 2012, Recherche de la signature radio de Encelade dans la magnétosphère de Saturne, doi:10.25935/j6a2-hp71, <https://doi.org/10.25935/j6a2-hp71>
- Warwick J. W., Pearce J. B., Peltzer R. G., Riddle A. C., 1977, Planetary radio astronomy experiment for Voyager missions, *Space Science Reviews*, *21*, 309
- Warwick J. W., et al., 1986, Voyager 2 Radio Observations of Uranus, *Science*, *233*, 102
- Wu C. S., 1985, Kinetic cyclotron and synchrotron maser instabilities - Radio emission processes by direct amplification of radiation, *Space Science Reviews*, *41*, 215
- Wu C. S., Lee L. C., 1979, A theory of the terrestrial kilometric radiation., *Astrophysical Journal*, *230*, 621
- Zarka P., Marques M. S., Louis C., Ryabov V. B., Lamy L., Echer E., Cecconi B., 2017, Radio emission from satellite-Jupiter interactions (especially Ganymede), in *Planetary Radio Emissions VIII*, eds Fischer, G. and Mann, G. and Panchenko, M. and Zarka, P., pp 45–58, doi:10.1553/PRE8s45
- Zarka P., Marques M. S., Louis C., Ryabov V. B., Lamy L., Echer E., Cecconi B., 2018, Jupiter radio emission induced by Ganymede and consequences for the radio detection of exoplanets, *Astronomy & Astrophysics*, *618*, A84